

# Length control of biodegradable fibre-like micelles via tuning solubility

O'Reilly, Rachel; Dove, Andrew; Foster, Jeff; Yu, Wei

DOI:

[10.1021/acs.macromol.9b02613](https://doi.org/10.1021/acs.macromol.9b02613)

License:

None: All rights reserved

Document Version

Peer reviewed version

Citation for published version (Harvard):

O'Reilly, R, Dove, A, Foster, J & Yu, W 2020, 'Length control of biodegradable fibre-like micelles via tuning solubility: a self-seeding Crystallization-Driven Self-Assembly of poly( $\epsilon$ -caprolactone) containing triblock copolymers', *Macromolecules*, vol. 53, no. 4, pp. 1514–1521. <https://doi.org/10.1021/acs.macromol.9b02613>

[Link to publication on Research at Birmingham portal](#)

## Publisher Rights Statement:

Length Control of Biodegradable Fiber-Like Micelles via Tuning Solubility: A Self-Seeding Crystallization-Driven Self-Assembly of Poly( $\epsilon$ -caprolactone)-Containing Triblock Copolymers, Wei Yu, Jeffrey C. Foster, Andrew P. Dove, and Rachel K. O'Reilly, *Macromolecules* 2020 53 (4), 1514-1521, DOI: 10.1021/acs.macromol.9b02613

## General rights

Unless a licence is specified above, all rights (including copyright and moral rights) in this document are retained by the authors and/or the copyright holders. The express permission of the copyright holder must be obtained for any use of this material other than for purposes permitted by law.

- Users may freely distribute the URL that is used to identify this publication.
- Users may download and/or print one copy of the publication from the University of Birmingham research portal for the purpose of private study or non-commercial research.
- User may use extracts from the document in line with the concept of 'fair dealing' under the Copyright, Designs and Patents Act 1988 (?)
- Users may not further distribute the material nor use it for the purposes of commercial gain.

Where a licence is displayed above, please note the terms and conditions of the licence govern your use of this document.

When citing, please reference the published version.

## Take down policy

While the University of Birmingham exercises care and attention in making items available there are rare occasions when an item has been uploaded in error or has been deemed to be commercially or otherwise sensitive.

If you believe that this is the case for this document, please contact [UBIRA@lists.bham.ac.uk](mailto:UBIRA@lists.bham.ac.uk) providing details and we will remove access to the work immediately and investigate.

# Length control of biodegradable fibre-like micelles *via* tuning solubility: a self-seeding Crystallization-Driven Self-Assembly of poly( $\epsilon$ -caprolactone) containing triblock copolymers

Wei Yu†, Jeffrey C. Foster§, Andrew P. Dove\*§ and Rachel K. O'Reilly\*§

†Department of Chemistry, University of Warwick, Gibbet Hill Road, Coventry, CV4 7AL, U.K.

§ School of Chemistry, University of Birmingham, Birmingham, B15 2TT, U.K.

**Abstract:** The Crystallization-Driven Self-Assembly of polymers based on semi-crystalline poly( $\epsilon$ -caprolactone) cores is currently an area of high interest on account of their well-known biocompatibility and biodegradability, yet a comprehensive understanding of coil-crystalline-coil type triblock copolymer assembly behaviour with respect to this core chemistry is yet to be realized. Herein, we demonstrate the simple preparation of well-defined tuneable 1D and 2D structures based on poly( $\epsilon$ -caprolactone) (PCL) triblock copolymers of different block ratios synthesized by ring-opening polymerisation (ROP) and reversible addition–fragmentation chain transfer (RAFT) polymerization. In this report, the assembly of PCL-based amphiphiles in various solvents was investigated to tune the morphology and size of the assemblies, with well-defined 2D platelets and long cylinders produced when using long, soluble coronal blocks or under good solvent conditions. By contrast, truncated short fibres were obtained for less soluble PCL-containing block copolymers or under poor solubility conditions for the core block as a consequence of the increasing amount of nuclei formed in the crystallization process. Furthermore, the length of PCL-based 1D nanostructures could be controlled by tuning self-assembly conditions, where the micelles' lengths varied from 93 to 1200 nm with narrow dispersities. This simple assembly methodology greatly simplifies the lengthy procedure required to prepare biodegradable 1D and 2D nanostructures from PCL with tuneable sizes, which demonstrate great potential as drug-delivery vehicles in the realm of biomedicine.

## Introduction

In the past few decades, the self-assembly of amphiphilic block copolymers (BCPs) in solution has offered an increasingly versatile bottom-up synthetic route to a wide range of nanoparticles with various microstructures and functionalities.<sup>1-5</sup> Recently, growing attention has been paid to the Crystallization-Driven Self-Assembly (CDSA) of block copolymers on account of the faculty to have access to well-defined 1D cylinders<sup>6-9</sup> and 2D platelets.<sup>10-13</sup> As a seeded-growth methodology for block copolymer crystallization in solution, living CDSA has emerged as a highly promising and versatile route to uniform core-shell micelles with control over dimension and architecture.<sup>14, 15</sup> In addition, this newly developed technique enables the achievement of intricate multi-component morphologies such as patchy or hollow rectangular platelets,<sup>16</sup> “cross-shaped” supermicelles,<sup>17</sup> non-centrosymmetric cylindrical micelles<sup>18</sup> and multidimensional hierarchical structures.<sup>19</sup>

In addition to the seeded-growth approach, self-seeding is also a commonly utilized strategy to control micelle size and dispersity using the CDSA process. In a typical self-seeded formulation, a semicrystalline block copolymer is suspended in a solvent and heated above its apparent dissolution temperature. Upon heating, the majority of the block copolymer dissolves, but a few crystallites survive. The heated solution is then cooled, and the solubilized unimers deposit on the nuclei, resulting in crystal growth to form cylindrical or platelet nanostructures. Semi-crystalline polymers such as poly(ferrocenyldimethylsilane) (PFS),<sup>20, 21</sup> poly(3-hexylthiophene) (P3HT),<sup>22</sup> poly(2-(perfluorooctyl)ethyl methacrylate (PFMA))<sup>23</sup> and polyethylene glycol (PEO)<sup>24</sup> have been exploited in this process, yielding uniform 1D or 2D micelles with controllable size by varying aging temperature, as higher temperatures increase the solubility of the unimers and reduce the overall proportion of seed crystals, leading to fewer and larger nanoparticles after cooling and aging. Apart from temperature, the solvent composition is also of great significance in the self-seeding process. For example, the size of uniform diamond lamellae obtained from poly(L-lactide)-*block*-polydimethyl acrylamide (PLLA-*b*-PDMA) diblock copolymers could be exquisitely tuned by varying the fraction of common solvent, a good solvent for core and corona block, used during self-assembly.<sup>25</sup> Similarly, increasing the fraction of good solvent was observed to decrease the fraction of undissolved crystal seeds during CDSA of

PFS-containing block copolymers, increasing the proportion of unimers and thus yielding larger aggregates.<sup>21</sup> Altogether, this self-seeding approach facilitates good control over a variety of CDSA systems.

Apart from the most widely studied CDSA block copolymer PFS,<sup>26</sup> additional semicrystalline polymers have been recently reported; for example,  $\pi$ -conjugated polymers poly(3-octylthiophene),<sup>27</sup> poly(phenylenevinylene)<sup>28</sup> and biodegradable polymers PLLA<sup>29-32</sup> and poly( $\epsilon$ -caprolactone) (PCL).<sup>33, 34</sup> PCL based diblock copolymers were demonstrated to assemble into cylinders and platelets *via* CDSA,<sup>35, 36</sup> and these assemblies were evidenced to undergo living seeded-growth to different lengths or dimensions with narrow size dispersities.<sup>37, 38</sup> Xu and co-workers also reported that the assembly morphology of PCL based diblock copolymers could be tuned from long cylindrical micelles to shorter ones or varied between 2D lamellae to 1D cylinders simply by adjusting coronal interactions, where corona repulsion could be manipulated to break large crystals into fragments.<sup>39, 40</sup> However, most of the CDSA studies regarding PCL focus on coil-crystalline diblock copolymers, with only one example referring to coil-crystalline-coil triblock copolymers.<sup>41</sup> In this report, Wang *et al.* investigated the effects of the block copolymer compositions on the micelle morphologies with diblock copolymers PCL-*b*-poly[2-(dimethylamino)ethyl methacrylate] (PCL-*b*-PDMAEMA), whereas a triblock counterpart PEO<sub>113</sub>-*b*-PCL<sub>62</sub>-*b*-PDMAEMA<sub>30</sub> was only studied for comparison.<sup>41</sup> Therefore, regarding triblock polymers with crystallizable middle block PCL, a deeper understanding of the CDSA process is still required and a general route to prepare crystalline nanoaggregates with those polymers has yet to be explored. Herein, we leverage knowledge gained from previous work in group regarding CDSA of PDMA-*b*-PLLA-*b*-PDMA triblock copolymers to study a new triblock system based on PCL. Whilst PLLA and PCL are superficially similar in their chemical structures, they possess remarkably different properties (i.e., thermal transition temperatures, crystal structures, degradation behaviour, etc.) and self-assembly behaviour, warranting an independent investigation into CDSA of PCL-based triblock copolymers.<sup>42</sup> We present a comprehensive CDSA study of PCL-based ABA type triblock copolymers, wherein PDMA was used as the stabilizer block. It was found that polymer composition determined the morphology and size of the corresponding assemblies, allowing access to hexagonal platelets or

cylindrical micelles with controllable dimensions. Furthermore, it was shown for the first time that CDSA could be conducted using PCL-based block copolymers *via* a self-seeding approach at room temperature, where the size of the micelles could be tuned by varying solvent composition. The methods developed in this work provide a simple and consistently reproducible protocol for the preparation of well-defined biodegradable 1D and 2D nanostructures, whose size and morphology are expected to facilitate applications in drug delivery, and tissue engineering.

## Results and discussion

A suite of triblock copolymers of PDMA<sub>x</sub>-*b*-PCL<sub>y</sub>-*b*-PDMA<sub>x</sub> with low dispersity ( $D_M < 1.2$ ) and varied block lengths (**Figure S1-S7** and **Table 1**) were synthesized by a combination of ring-opening polymerization (ROP) and reversible addition–fragmentation chain transfer (RAFT) polymerization (**Scheme S1**) following methodology reported by our group.<sup>29</sup>

**Table 1.** Characterisation of PDMA<sub>x</sub>-*b*-PCL<sub>y</sub>-*b*-PDMA<sub>x</sub> triblock copolymers with varying core and corona lengths.

Triblock copolymer	Entry	$M_{n,NMR}^a$ (kDa)	$M_{n,SEC}^b$ (kDa)	$D_M^b$	Solvophobic content (wt%) <sup>c</sup>
PDMA <sub>40</sub> - <i>b</i> -PCL <sub>30</sub> - <i>b</i> -PDMA <sub>40</sub>	<b>T1</b>	10.7	13.5	1.09	32
PDMA <sub>96</sub> - <i>b</i> -PCL <sub>30</sub> - <i>b</i> -PDMA <sub>96</sub>	<b>T2</b>	22.8	27.4	1.15	15
PDMA <sub>150</sub> - <i>b</i> -PCL <sub>30</sub> - <i>b</i> -PDMA <sub>150</sub>	<b>T3</b>	34.2	38.4	1.18	10
PDMA <sub>47</sub> - <i>b</i> -PCL <sub>40</sub> - <i>b</i> -PDMA <sub>47</sub>	<b>T4</b>	14.3	18.1	1.13	32
PDMA <sub>124</sub> - <i>b</i> -PCL <sub>40</sub> - <i>b</i> -PDMA <sub>124</sub>	<b>T5</b>	30.4	36.2	1.14	15
PDMA <sub>203</sub> - <i>b</i> -PCL <sub>40</sub> - <i>b</i> -PDMA <sub>203</sub>	<b>T6</b>	44.6	48.3	1.17	10
PDMA <sub>75</sub> - <i>b</i> -PCL <sub>60</sub> - <i>b</i> -PDMA <sub>75</sub>	<b>T7</b>	21.4	25.3	1.08	32
PDMA <sub>190</sub> - <i>b</i> -PCL <sub>60</sub> - <i>b</i> -PDMA <sub>190</sub>	<b>T8</b>	45.6	49.3	1.13	15
PDMA <sub>302</sub> - <i>b</i> -PCL <sub>60</sub> - <i>b</i> -PDMA <sub>302</sub>	<b>T9</b>	68.4	71.3	1.18	10

<sup>a</sup> Calculated by <sup>1</sup>H NMR spectroscopy (400 MHz, CDCl<sub>3</sub>). <sup>b</sup> Measured by SEC (DMF with 5 mM NH<sub>4</sub>BF<sub>4</sub>, PMMA standards). <sup>c</sup> PCL weight fraction in the PDMA<sub>y</sub>-*b*-PCL<sub>x</sub>-*b*-PDMA<sub>y</sub> triblock copolymers was calculated by <sup>1</sup>H NMR spectroscopy.

It was previously demonstrated that PCL-*b*-PDMA diblock copolymers could yield cylindrical morphologies by carrying out CDSA in a single alcoholic solvent after a heating-cooling process.<sup>37</sup>

Meanwhile, in the case of PLLA based block copolymers, it was also found that coil-crystalline-coil architectures ( $\text{PDMA}_x\text{-}b\text{-PLLA}_y\text{-}b\text{-PDMA}_x$ ) could improve polymer solubility in comparison to its diblock coil-crystalline counterpart ( $\text{PLLA}_y\text{-}b\text{-PDMA}_x$ ), thus allowing CDSA merely by dissolving and aging at room temperature.<sup>37</sup> Analogous to this, the system used in this report also uses PDMA corona chemistry, however it relies on an alternative polyester block – PCL. Based upon the similarity in overall block copolymer structure, it was hypothesized that this room temperature assembly methodology would also be applicable to our PCL triblock system. Therefore, a series of alcoholic solvents (*i.e.* methanol, ethanol, 1-propanol, 1-butanol) were screened for CDSA of  $\text{PDMA}_x\text{-}b\text{-PCL}_y\text{-}b\text{-PDMA}_x$  at room temperature. Triblock copolymers could be dissolved in methanol, ethanol, 1-propanol and 1-butanol (5 mg mL<sup>-1</sup>), with a weak Tyndall effect observed for the polymer solutions. For example, during the assembly of **T5**, the solutions gradually became turbid after aging for two days at room temperature, which suggested the formation of larger aggregates (**Figure 1**).<sup>29</sup> Transmission electron microscopy (TEM) analysis of the assembly solutions showed that cylindrical micelles were obtained from all the alcoholic solvents listed above. To be specific, in methanol, very long micelles (> 4  $\mu\text{m}$ ) were observed (**Figure S8a**) and proved to be crystalline by Wide Angle X-ray Scattering analysis (**Figure S9**), whilst changing the assembly solvent to a less polar alcoholic solvent (*i.e.* ethanol) yielded long nanoparticles (>4  $\mu\text{m}$ ) mixed with short ones (0.5-4  $\mu\text{m}$ ) (**Figure S8b**). Furthermore, when the less polar solvents were used (1-propanol and 1-butanol), much shorter nanoparticles were observed (< 2  $\mu\text{m}$ ) (**Figure S8 c and d**). Based on these initial results, the self-assembly process was postulated to occur as follows (**Figure 1**): at first, most of the polymer chains are dissolved as unimers in the alcoholic solvent, with the remaining insoluble polymers forming crystal nuclei. Subsequently, free polymer chains deposited on these nuclei, evolving into larger crystallites (*i.e.* crystalline cylinders) upon aging of the samples. Solvent quality plays a vital role in the CDSA process. Increased unimer solubility: (1) limits the proportion of nuclei in the assembly solution; and (2) increases the mobility of the crystallizable PCL core-forming block, favouring its deposition on the growing crystal front over the creation of new nuclei or aggregation (*i.e.*, micelle formation). This explains why long cylinders are obtained in methanol (a good solvent for the semi-crystalline PCL blocks) and short cylinders from 1-butanol.

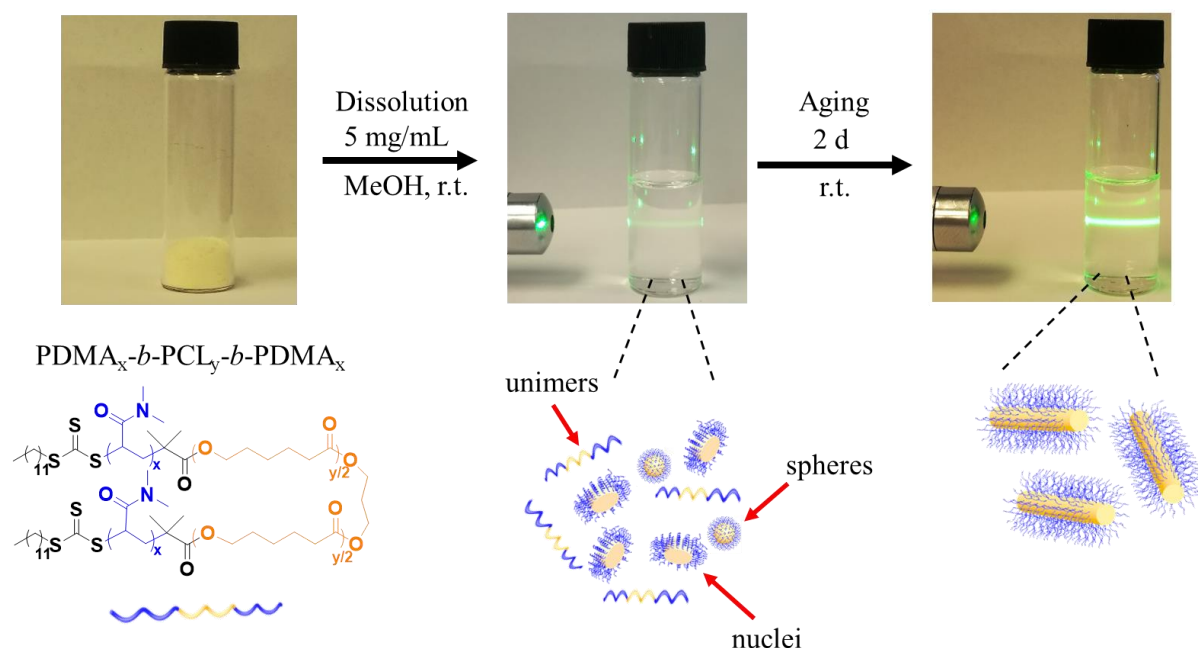


**Figure 1.** Schematic representation of the preparation of crystalline micelles by PDMA<sub>x</sub>-b-PCL<sub>y</sub>-b-PDMA<sub>x</sub> triblock copolymer: polymer powder was dissolved into methanol at 5 mg mL<sup>-1</sup> at r.t. (25 °C). Initially, the Tyndall effect is very weak, which indicated that the majority of polymer was solubilized. After aging for two days at r.t., the Tyndall effect was much stronger, suggesting the formation of more or larger cylinders.

To further confirm the assumption that unimer solubility influenced the micelle length, assembly in mixed solvents of varying proportions was tested. It was known from the above work that methanol is a good solvent for the polymer, whereas water doesn't solubilize polymer **T5** at room temperature (5 mg mL<sup>-1</sup>) (**Figure S10**). Therefore, polymer **T5** was assembled under the same conditions *i.e.* 5 mg mL<sup>-1</sup> at room temperature but in different solvent systems (20-40 v/v %, H<sub>2</sub>O in MeOH). After aging for two days, TEM analysis (**Figure 2c** and **Figure S11**) revealed that a 20 v/v % H<sub>2</sub>O in MeOH resulted in the formation of cylindrical micelles, but a dramatic decrease in the micelle length ( $L_n = 270$  nm) was observed in comparison to the 100% methanol sample ( $L_n > 4$  μm, **Figure 2b**). These data support the assumption that decreased micelle length for our triblock copolymer system was caused by lower unimer solubility, thus leading to a larger proportion of seeds (**Figure 2a**). In addition, as the water ratio was further increased to 30 v/v % and 40 v/v %, the micelles became even shorter, with average lengths of *ca.* 95 nm and 55 nm, respectively (**Figure 2d, e** and **Figure S11**).

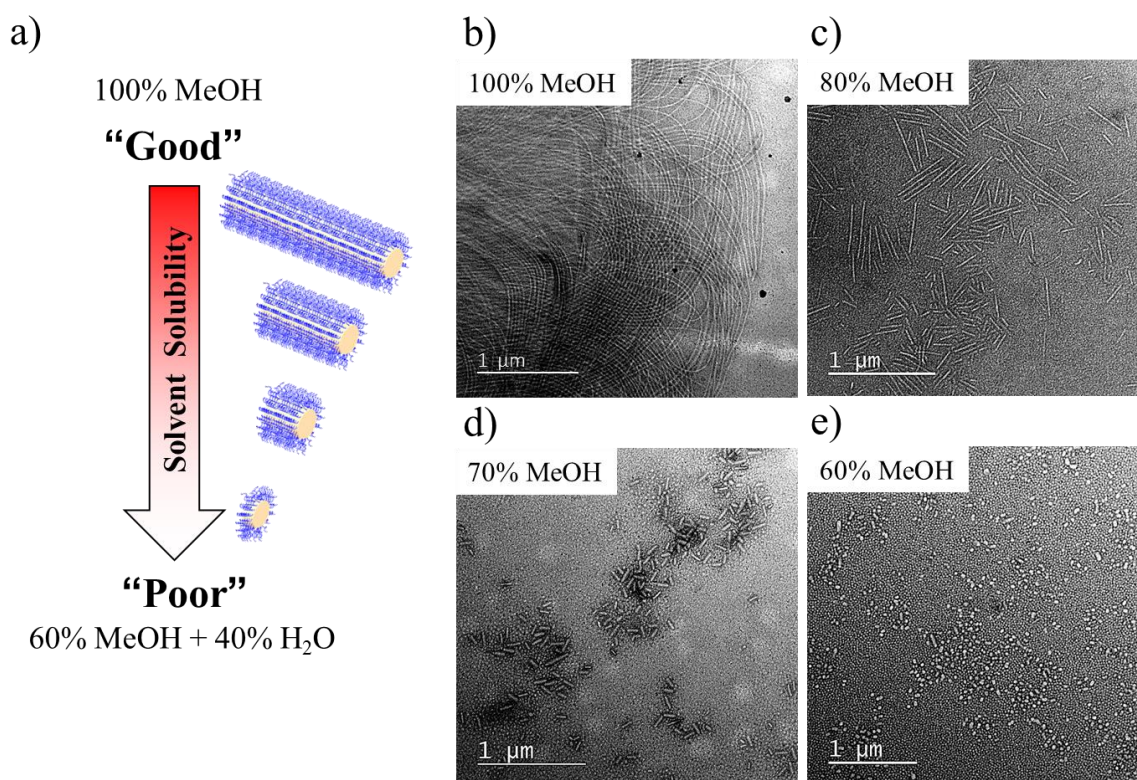


**Figure 2.** a) Schematic representation of the assembly of micelles achieved from polymer **T5** in methanol/water mixed solvents with different ratios at 5 mg mL<sup>-1</sup> and aged at r.t. for two days. TEM micrographs of **T5** assembled in b) 100 vol % methanol, c) 20 v/v % H<sub>2</sub>O in MeOH, d) 30 v/v % H<sub>2</sub>O in MeOH e) 40 v/v % H<sub>2</sub>O in MeOH. Samples were negatively stained using a uranyl acetate solution (0.5 w/v %).

Since the cylindrical micelles obtained were reasonably uniform and the assembly solution was solubilized initially, the “self-seeding” CDSA process was assumed to be occurring in this system. To validate this assumption, a kinetic self-assembly study was performed with polymer **T5**, using standard assembly conditions (5 mg mL<sup>-1</sup> in methanol at r.t.). An aliquot was taken from the assembly solution after 0 h, 3 h and 24 h aging time, respectively, for TEM inspection. Surprisingly, spherical micelles were exclusively observed on the TEM grid initially (**Figure 3a, 0 h**). However, as the aging time increased, short cylinders began to emerge (**Figure 3b**), and by 24 h, longer fibres (**Figure 3c**) were observed. The assembly process was also monitored *in situ* by dynamic light scattering (DLS). To keep consistency, the assembly condition applied here is the same as TEM inspection (polymer **T5**, in methanol, 5 mg mL<sup>-1</sup>). Mean count rate refers to the actual average number of photons per second arriving at the detector, namely scattering intensity. It was found that in the initial stages the mean count rate was low, 212 kilo counts per second (kcps), indicating the absence of large aggregates. However,

as the aging time evolved (10 min intervals for signal collection), the mean count rate continuously rose up to 988 kcps at 24 h (**Figure 3d**), suggesting the formation of assemblies gradually. Considering the aggregate size distribution averaged by intensity, signals below 50 nm were assigned to unimers or spheres, and higher average size values were assumed to be aggregates (**Figure 3e**). During the kinetic experiments, the intensity % of distribution in large size area and the average sizes continuously increased in the process, consistent with the fact observed by TEM that large cylinders gradually formed over time. Microdifferential scanning calorimetry ( $\mu$ DSC) analysis was applied to further corroborate our assumption. Here, the assembly solution (polymer **T5**, 5 mg mL<sup>-1</sup> in methanol) showed no melting peak after dissolution, whereas a sharp peak around 27 °C was observed after aging for three hours and a melting peak with higher intensity was further evidenced after one day (**Figure 3f**). These results proved the absence of large crystalline aggregates at first and the growth of the crystalline structures afterward, which strongly supports the presumed self-seeded assembly process. Slightly different from our initial assumption of self-seeded growth, these kinetic experiments further established that these polymers were not only molecularly dissolving into unimers, while leaving a few nuclei, but also formed spherical micelles. These spheres can be considered as a reservoir of unimers that gradually release free polymer chains into the assembly solution. During the progression of the crystallization, unimers were continuously deposited on the growing crystal front (**Figure 3g**). Thus, the amount of spherical micelles diminished accordingly to replenish the consumed unimers. In addition to the example polymer (**T5**), the coexistence of spheres and cylinders (or lamellae) was also observed in the other assembly tests in their initial assembly stages, such as for polymer **T6** and **T4** (aging for 3 h, **Figure S12a** and **c**). Similarly, the proportion of spherical micelles declined considerably as the assembly solutions were aged longer (1 day, **Figure S12b** and **d**).

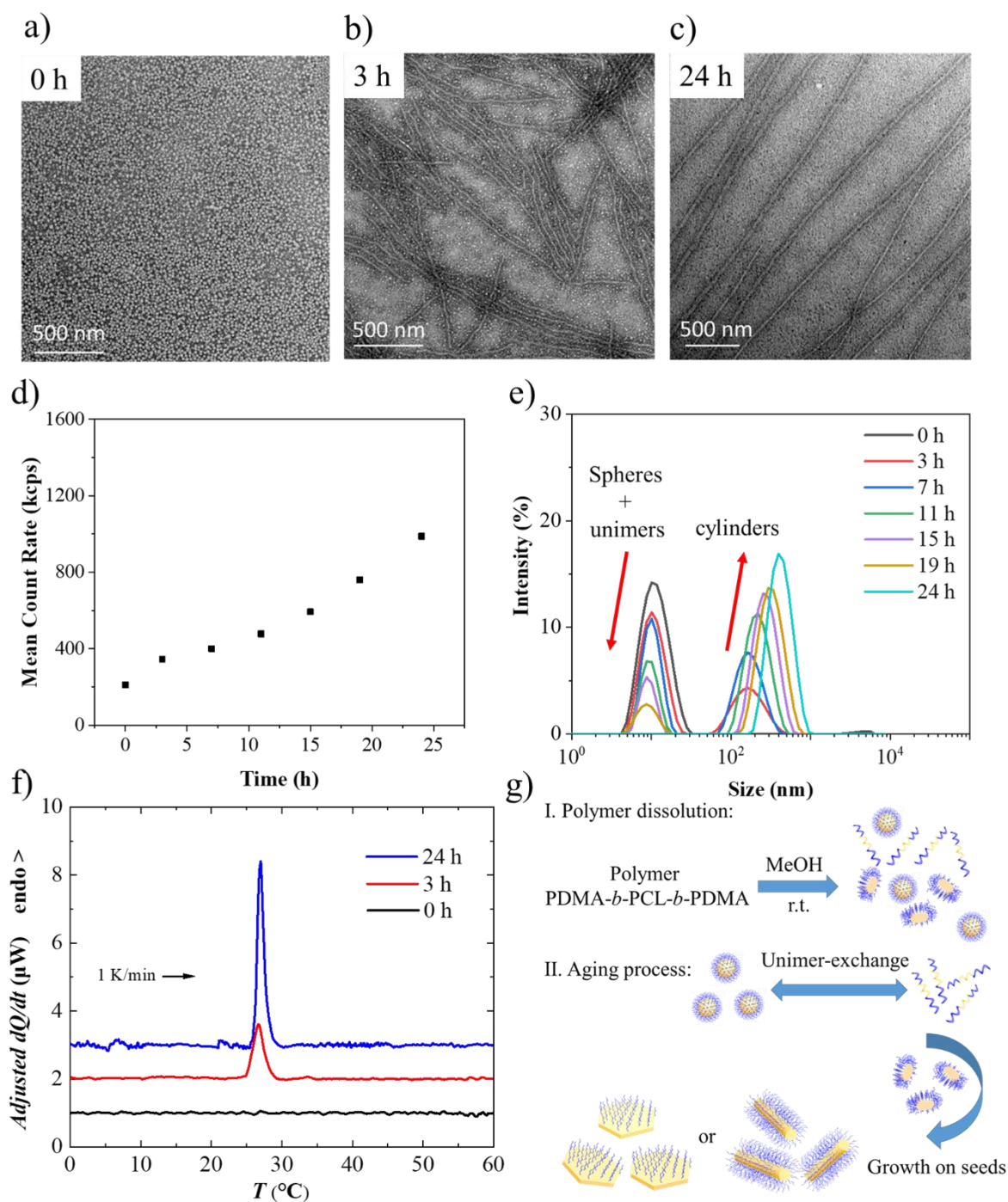


**Figure 3.** TEM micrographs of the micelles achieved from polymer **T5** in methanol (5 mg mL<sup>-1</sup>) at r.t.: a) 0 h b) 3 h c) 24 h. Samples were negatively stained using uranyl acetate (0.5 w/v %). d) Mean count rate monitored from assembly solution, polymer **T5** 5 mg mL<sup>-1</sup> in methanol at r.t. *in situ* with a measurement interval of 10 min e) Size distribution averaged by intensity over the same time period. Each measurement was repeated five times. f)  $\mu$ DSC heating traces of a 5 mg mL<sup>-1</sup> in methanol solution of polymer **T5**, the assembly samples were analysed after aging for 0 h, 3 h and 24 h at r.t. The scanning rate is 1 K min<sup>-1</sup>. g) Schematic representation of the preparation of crystalline micelles from a PDMA<sub>x</sub>-*b*-PCL<sub>y</sub>-*b*-PDMA<sub>x</sub> triblock copolymer.

Although the kinetics of the assemblies' formation from polymers **T4**, **T5** and **T6** are similar as mentioned above, the obtained micelle sizes or morphologies were different as a consequence of the

variation in corona block lengths. In order to understand how the block length and ratio of PCL based triblock copolymers influenced their CDSA behaviour, a series of PDMA<sub>x</sub>-*b*-PCL<sub>y</sub>-*b*-PDMA<sub>x</sub> triblock copolymers (**T1-T9**) were synthesized and assembled under the standard conditions (5 mg mL<sup>-1</sup> in methanol, r.t.). After aging for two days, TEM analysis (**Figure 4**) was performed to visualize the obtained morphologies.

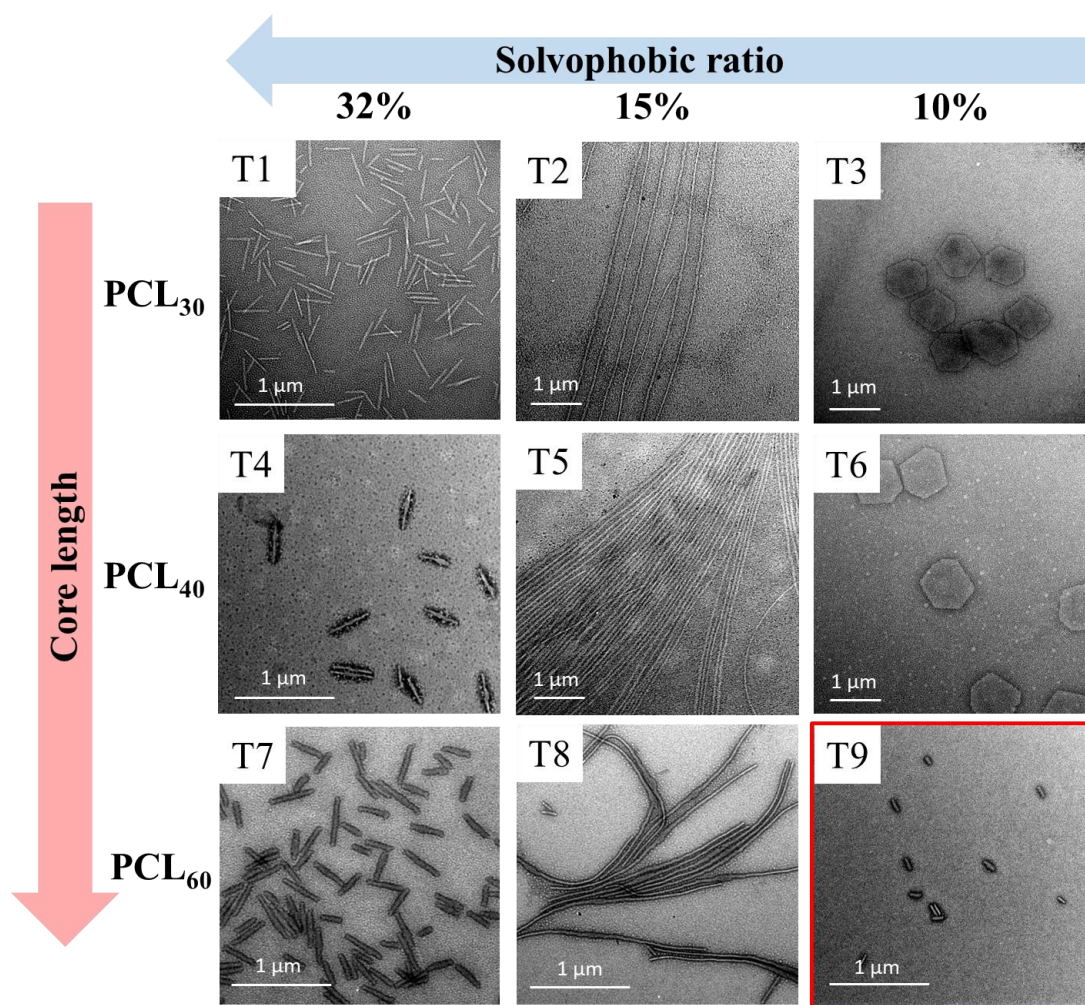


**Figure 4.** TEM micrographs of the micelles obtained from polymers PDMA<sub>x</sub>-*b*-PCL<sub>y</sub>-*b*-PDMA<sub>x</sub> assembled in methanol (5 mg mL<sup>-1</sup>) and aged at r.t. for two days: **T1-T9**. Samples were negatively stained using a uranyl acetate solution (0.5 w/v %).

For PDMA<sub>x</sub>-*b*-PCL<sub>y</sub>-*b*-PDMA<sub>x</sub> with a core block length of DP<sub>PCL</sub> = 40, a longer corona (DP<sub>PDMA</sub> = 400, polymer **T6**) resulted in the formation of 2D hexagonal platelets (**Figure 4, T6**), whereas its shorter counterpart (DP<sub>PDMA</sub> = 250, polymer **T5**) formed long fibres (**Figure 4, T5**). Studies on the formation of di- and tri-BCP micelles with PLLA cores and PDMA coronas have also revealed a preference for 2D lamellae over 1D cylinders when the percentage composition of corona-forming block was

increased.<sup>29</sup> A likely explanation could be that the increased solubility of the polymer with longer corona length gives adequate time for the semi-crystalline polymer chain to adopt a preferred crystal conformation, thus leading to well-defined structures (2D platelets).<sup>43</sup> Indeed, unimer composition (and thus its solubility in the assembly medium) has been implicated as a governing factor for morphological evolution during CDSA, as evidenced by its impact on crystallization kinetics in related systems.<sup>43</sup> This rationale sufficiently explains the trends in assembly of **T5** and **T6**. More interestingly, when the solvophobic ratio was further increased to 32% (polymer **T4**), much shorter cylinders (**Figure 4, T4**) were obtained, in line with the concept that better solubility leads to the preferred crystal morphology.

Since varying the corona block was confirmed to influence CDSA morphology, the impact of altering core block length was then investigated. The length of the core block was reduced from PCL<sub>40</sub> to PCL<sub>30</sub> to probe the influence of a shorter core block (polymer **T1-T3**) on the assembly behaviour, while the same solvophobic ratios were maintained. Under the standard assembly conditions, the obtained morphologies were quite similar to the PCL<sub>40</sub>: the longest corona (polymer **T3**) led to 2D hexagonal platelets, the intermediate corona (polymer **T2**) produced hairy cylinders and the shortest corona (polymer **T1**) formed short fibres (**Figure 4, T1-T3**). In contrast, as the core block length was extended to DP<sub>PCL</sub> = 60 (polymer **T7-T9**), the obtained micelles followed a slightly different trend. To be specific, polymer **T7** assembled into short cylinders showing similar length ( $L_n = 200$  nm) to **T4** ( $L_n = 280$  nm, same solvophobic ratio 32%). However, the nanoparticles obtained from **T8** were much shorter ( $L_n = 820$  nm) than those of **T5** ( $L_n > 4$   $\mu$ m). More surprisingly, as the corona length was further increased to DP<sub>PDMA</sub> = 600 (polymer **T9**), short fibres ( $L_n = 84$  nm, **Figure 4, T9**) were achieved instead of platelets. These differences can be rationalized in view of the similar system (PDMA<sub>x</sub>-b-PLLA<sub>y</sub>-b-PDMA<sub>x</sub>) reported before: though the block ratios of the PCL<sub>60</sub> series are similar to the PCL<sub>40</sub> counterparts, the longer core block for the PCL<sub>60</sub> samples decreased their overall solubility, impeding the formation of the favoured conformation (lamellae structure) during the crystallization process.<sup>29</sup> It is worth noting that the assemblies obtained from coil-crystalline-coil triblock copolymers PDMA<sub>x</sub>-b-PCL<sub>y</sub>-b-PDMA<sub>x</sub> by the single component solution-phase approach showed remarkable uniformity. Indeed, the length dispersity ( $L_w/L_n$ ) of the cylindrical micelles (assemblies of polymer **T1, T4, T7, T8** and **T9**) and the

area dispersity of the platelets (nanoparticles from polymer **T3** and **T6**) were all controlled below 1.10 (**Table S1, S2** and **Figure S13**).

As mentioned above, in the PCL-based triblock copolymer system, the polymer dissolution process consumed most of the crystalline domains leaving a few ordered nuclei and spherical micelles to initiate nanoparticle growth. Interestingly, as a consequence of the particular polymer composition and solvent conditions, this self-seeding process could be realized without any heating in a single solvent. Similar assembly behaviour has previously been observed in PLLA based triblock copolymer systems, where it was shown that uniform diamond platelets could be fabricated at room temperature in methanol.<sup>25</sup> In order to further corroborate the hypothesis of a self-seeding process, assembly solution containing PDMA<sub>302</sub>-*b*-PCL<sub>60</sub>-*b*-PDMA<sub>302</sub> (Polymer **T9**) was annealed at 28, 31, 35 or 40 °C for 1 h before cooling to room temperature (25 °C) and aging for two days. TEM analysis of the annealed samples at 28 and 31 °C showed longer micelles (*ca.* 130 and 240 nm, **Figure 5a** and **b**) compared to 25 °C ( $L_n = 84$  nm), with narrow length distributions ( $L_w/L_n < 1.10$ , **Figure S14** and **Table S3**). As the aging temperature was increased to 35 °C and 40 °C, the obtained fibres were even longer (*ca.* 430 and 1200 nm, **Figure 5c** and **d**) with similarly low length dispersity ( $L_w/L_n < 1.10$ , **Figure S14** and **Table S3**). Based on the initial length of the seeds at 25 °C and the final length of micelles after annealing, the fraction of surviving fragments were calculated at each annealing temperature (see SI).<sup>20</sup> As shown in **Figure 5f**, in the range of 25–40 °C, the fraction of surviving seeds decreased exponentially with increasing temperature, a key characteristic of a self-seeding process.<sup>21, 23</sup> Indeed, if the annealing temperature was too high (e.g., 45 °C, which is far above the melting temperature of PCL in methanol (**Figure 3f**), spheres were obtained instead (**Figure S15**). This was presumably because all the crystalline nuclei had melted at that temperature and, upon cooling, the unimers assembled into spherical micelles since there was no crystal front available to initiate the crystallization. Mei *et al.* also observed a similar result in their poly(2-vinylpyridine)-*b*-PCL diblock copolymer assembly system, when crystalline lamellae were achieved at 20 °C and amorphous spheres were obtained at higher temperature (30 °C).<sup>44</sup>

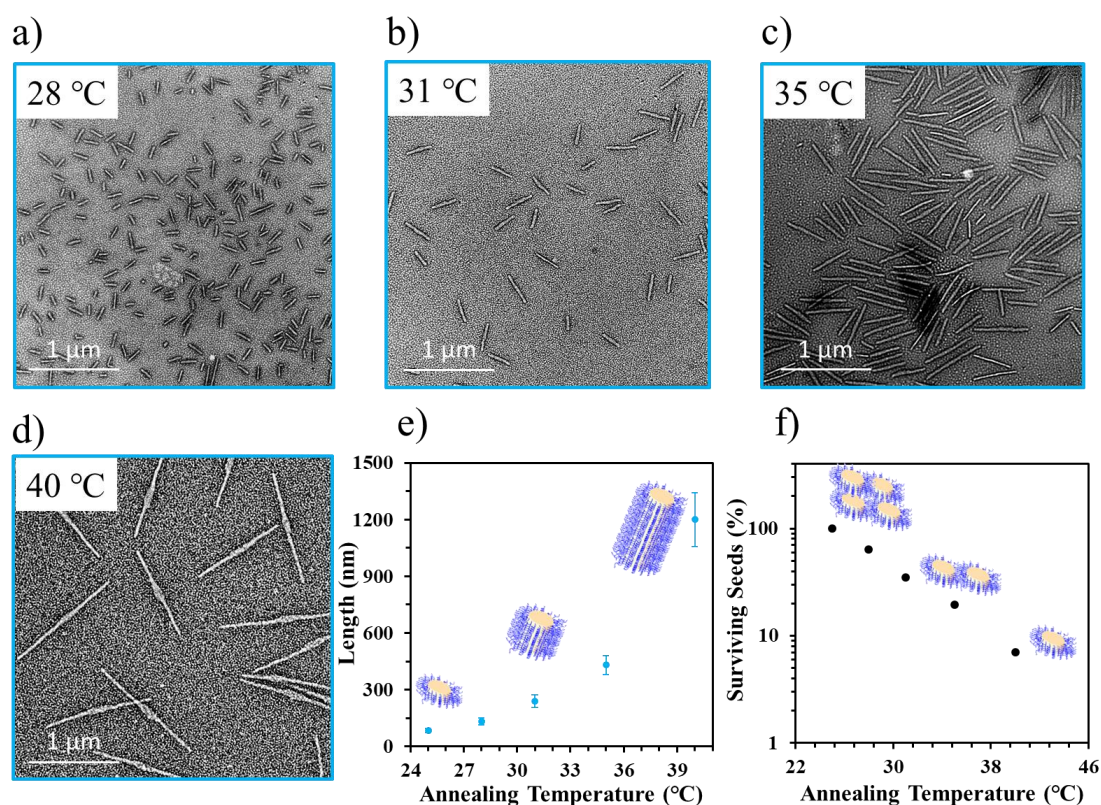


**Figure 5.** TEM micrographs of PDMA<sub>302</sub>-*b*-PCL<sub>60</sub>-*b*-PDMA<sub>302</sub> self-assembled in methanol at 5 mg mL<sup>-1</sup> following annealing at a) 28 °C b) 31 °C c) 35 °C and d) 40 °C for 1 hour before cooling down to r.t. (25 °C) and aging for two days. Samples were negatively stained using a uranyl acetate solution (0.5 w/v %). e) Number-average micelle length  $L_n$  versus annealing temperature calculated from particle analysis based TEM images. In each case, at least 100 particles were analysed. f) Semi-logarithmic plots of fraction of surviving seeds in solution versus annealing temperatures.

In addition to the influence of temperature, the effect of solvent on the number of remaining seeds was also investigated. To be specific, polymer **T9** was assembled under similar conditions to previous experiments (5 mg mL<sup>-1</sup>, r.t. aging for 2 d) but in mixtures of THF and methanol. It was found that a small amount of “good solvent” for the core block (4 v/v % THF in MeOH) promoted an increase in micelle length from 84 nm to 260 nm ( $L_w/L_n < 1.1$ , **Figure 6a**). Furthermore, as the THF content was increased from 6 to 8 to 10 v/v % THF in MeOH, the cylindrical micelles grew to 345, 500 and 760 nm in length, respectively (**Figure 6b-e**), with low dispersity ( $L_w/L_n < 1.1$ , **Table S4** and **Figure S16**). The fraction of surviving seeds versus the THF content of the initial solutions was calculated based on the initial length of the seeds in 100% methanol and the final length of the micelles in the mixed solution (**Figure 6f**). It was found that as the THF content of the solutions increased from 4 to 10 vol %, the fraction of surviving seeds decreased. Moreover, spherical micelles were exclusively obtained when the good solvent proportion (THF) was further increased to 15% (**Figure S17**). Similar to before, 15 vol %

THF likely dissolves all the crystalline nuclei, impeding crystallization. In general, the addition of common solvent or heating of the solution were both used to manipulate the number of seeds in the assembly solution, making it possible to tune the resultant cylindrical micelle length (**Figure 6g**).

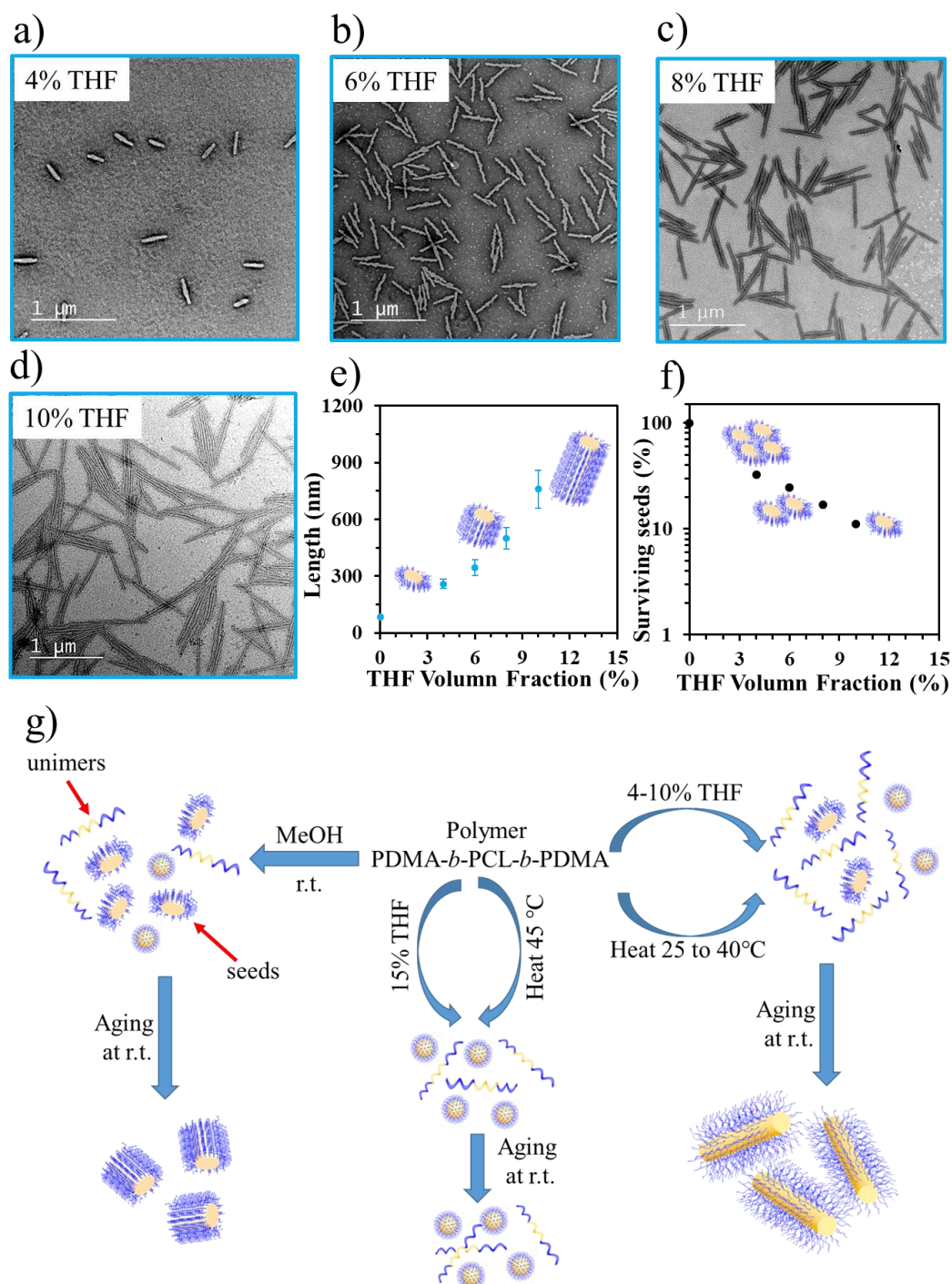


**Figure 6.** TEM micrographs of PDMA<sub>302</sub>-*b*-PCL<sub>60</sub>-*b*-PDMA<sub>302</sub> self-assembled in a) 4 v/v % THF in MeOH b) 6 v/v % THF in MeOH c) 8 v/v % THF in MeOH d) 10 v/v % THF in MeOH 5 mg mL<sup>-1</sup> and aged at r.t. for two days. Samples were negatively stained using a uranyl acetate solution (0.5 w/v %). e) Number-average micelle length  $L_n$  versus volume fraction of THF in the assembly solution,

calculated from particle analysis using TEM images. In each case, at least 100 particles were analysed. f) Plots of fraction of surviving seeds in solution of PDMA<sub>302</sub>-*b*-PCL<sub>60</sub>-*b*-PDMA<sub>302</sub> versus the volume fraction of THF. g) Schematic representation of the preparation of near monodisperse fibres by self-seeding method.

## Conclusion

In summary, the systematic CDSA study of PDMA<sub>x</sub>-*b*-PCL<sub>y</sub>-*b*-PDMA<sub>x</sub> triblock copolymers to prepare crystalline poly( $\epsilon$ -caprolactone) assemblies *via* a simple, single component solution-phase methodology at room temperature is reported, which greatly simplifies access to well-defined 1D and 2D organic nanoparticles. It was further demonstrated that the solubility of the copolymers could be exploited to control the size and morphology of the nanoparticles, which was mainly attributed to two factors: the block ratio and solvent quality. In accordance with recent reports of poly(ester) crystalline nanoparticles, good solvent quality and large corona-core ratios facilitated the formation of crystalline micelles with fewer defects, such as 2D platelets or long cylindrical micelles, whereas the opposite parameters resulted in short cylinders. Furthermore, it was shown that the cylinder length (84 nm to 1200 nm) of PCL-based triblock copolymers could be controllably manipulated by adjusting the ratio of dissolved unimer to nuclei through the variation of solvent composition and/or temperature. The ability to readily access and control the assembly of PCL-based triblock copolymers into spherical, cylindrical or lamellar micelles with uniform sizes through a simple assembly approach provides a platform to develop a series of new materials with more complexity such as ABC type terpolymers, which show great potential for future bio-relevant applications.

## AUTHOR INFORMATION

### Corresponding Authors

\* Email: [a.dove@bham.ac.uk](mailto:a.dove@bham.ac.uk)

\* Email: [r.oreilly@bham.ac.uk](mailto:r.oreilly@bham.ac.uk)

### ORCID

Jeffrey Foster: [0000-0002-1043-7172](https://orcid.org/0000-0002-1043-7172)

Andrew Dove: [0000-0001-8208-9309](https://orcid.org/0000-0001-8208-9309)

Rachel O'Reilly: [0000-0002-1043-7172](https://orcid.org/0000-0002-1043-7172)

## Authors Contribution

The manuscript was written through contributions of all authors. All authors have given approval to the final version of the manuscript.

## Notes

The authors declare no competing financial interest.

## ACKNOWLEDGMENTS

The authors thank the University of Warwick, University of Birmingham, China Scholarship Council (W.Y.) for research funding. The authors thank Yujie Xie for designing the scheme.

## ASSOCIATED CONTENT

The Supporting Information is available free of charge on the ACS Publications website at DOI: 10.1021/acs.macromol.xxxxxxx.

Additional characterization results including materials, experimental procedures, characterization techniques, and additional data (SEC, NMR, TEM, and WAXS).

## REFERENCE:

1. He, W.-N.; Xu, J.-T. Crystallization assisted self-assembly of semicrystalline block copolymers. *Prog. Polym. Sci.* **2012**, 37 (10), 1350-1400.
2. Mai, Y.; Eisenberg, A. Self-assembly of block copolymers. *Chem. Soc. Rev.* **2012**, 41 (18), 5969-5985.
3. Chen, G.; Jiang, M. Cyclodextrin-based inclusion complexation bridging supramolecular chemistry and macromolecular self-assembly. *Chem. Soc. Rev.* **2011**, 40 (5), 2254-2266.
4. Ge, Z.; Liu, S. Functional block copolymer assemblies responsive to tumor and intracellular microenvironments for site-specific drug delivery and enhanced imaging performance. *Chem. Soc. Rev.* **2013**, 42 (17), 7289-7325.
5. Blanz, A.; Armes, S. P.; Ryan, A. J. Self-Assembled Block Copolymer Aggregates: From Micelles to Vesicles and their Biological Applications. *Macromol. Rapid Commun.* **2009**, 30 (4), 267-277.
6. Xu, J.; Zhou, H.; Yu, Q.; Manners, I.; Winnik, M. A. Competitive Self-Assembly Kinetics as a Route To Control the Morphology of Core-Crystalline Cylindrical Micelles. *J. Am. Chem. Soc.* **2018**, 140 (7), 2619-2628.
7. Schmelz, J.; Schedl, A. E.; Steinlein, C.; Manners, I.; Schmalz, H. Length control and block-type architectures in worm-like micelles with polyethylene cores. *J. Am. Chem. Soc.* **2012**, 134 (34), 14217-14225.
8. Hudson, Z. M.; Qian, J.; Boott, C. E.; Winnik, M. A.; Manners, I. Fluorous Cylindrical Micelles of Controlled Length by Crystallization-Driven Self-Assembly of Block Copolymers in Fluorinated Media. *ACS Macro Lett.* **2015**, 4 (2), 187-191.
9. Oliver, A. M.; Gwyther, J.; Winnik, M. A.; Manners, I. Cylindrical Micelles with "Patchy" Coronas from the Crystallization-Driven Self-Assembly of ABC Triblock Terpolymers with a Crystallizable Central Polyferrocenyldimethylsilane Segment. *Macromolecules* **2017**, 51 (1), 222-231.
10. He, X.; He, Y.; Hsiao, M. S.; Harniman, R. L.; Pearce, S.; Winnik, M. A.; Manners, I. Complex and Hierarchical 2D Assemblies via Crystallization-Driven Self-Assembly of Poly(l-lactide) Homopolymers with Charged Termini. *J. Am. Chem. Soc.* **2017**, 139 (27), 9221-9228.
11. He, X.; Hsiao, M.-S.; Boott, C. E.; Harniman, R. L.; Nazemi, A.; Li, X.; Winnik, M. A.; Manners, I. Two-dimensional assemblies from crystallizable homopolymers with charged termini. *Nat. Mater.* **2017**, 16 (4), 481-491.

12. Nazemi, A.; He, X.; MacFarlane, L. R.; Harniman, R. L.; Hsiao, M. S.; Winnik, M. A.; Faul, C. F.; Manners, I. Uniform "Patchy" Platelets by Seeded Heteroepitaxial Growth of Crystallizable Polymer Blends in Two Dimensions. *J. Am. Chem. Soc.* **2017**, 139 (12), 4409-4417.
13. Hudson, Z. M.; Boott, C. E.; Robinson, M. E.; Rupar, P. A.; Winnik, M. A.; Manners, I. Tailored hierarchical micelle architectures using living crystallization-driven self-assembly in two dimensions. *Nat. Chem.* **2014**, 6 (10), 893-900.
14. Wang, X.; Guerin, G.; Wang, H.; Wang, Y.; Manners, I.; Winnik, M. A. Cylindrical block copolymer micelles and co-micelles of controlled length and architecture. *Science* **2007**, 317 (5838), 644-647.
15. Boott, C. E.; Leita, E. M.; Hayward, D. W.; Laine, R. F.; Mahou, P.; Guerin, G.; Winnik, M. A.; Richardson, R. M.; Kaminski, C. F.; Whittell, G. R.; Manners, I. Probing the Growth Kinetics for the Formation of Uniform 1D Block Copolymer Nanoparticles by Living Crystallization-Driven Self-Assembly. *ACS Nano* **2018**, 12 (9), 8920-8933.
16. Qiu, H.; Gao, Y.; Boott, C. E.; Gould, O. E.; Harniman, R. L.; Miles, M. J.; Webb, S. E.; Winnik, M. A.; Manners, I. Uniform patchy and hollow rectangular platelet micelles from crystallizable polymer blends. *Science* **2016**, 352 (6286), 697-701.
17. Li, X.; Gao, Y.; Boott, C. E.; Hayward, D. W.; Harniman, R.; Whittell, G. R.; Richardson, R. M.; Winnik, M. A.; Manners, I. "Cross" Supramicelles via the Hierarchical Assembly of Amphiphilic Cylindrical Triblock Comicelles. *J. Am. Chem. Soc.* **2016**, 138 (12), 4087-4095.
18. Rupar, P. A.; Chabanne, L.; Winnik, M. A.; Manners, I. Non-centrosymmetric cylindrical micelles by unidirectional growth. *Science* **2012**, 337 (6094), 559-562.
19. Qiu, H.; Hudson, Z. M.; Winnik, M. A.; Manners, I. Multidimensional hierarchical self-assembly of amphiphilic cylindrical block comicelles. *Science* **2015**, 347 (6228), 1329-1332.
20. Qian, J.; Guerin, G.; Lu, Y.; Cambridge, G.; Manners, I.; Winnik, M. A. Self-seeding in one dimension: an approach to control the length of fiberlike polyisoprene-polyferrocenylsilane block copolymer micelles. *Angew. Chem. Int. Ed.* **2011**, 50 (7), 1622-1625.
21. Qian, J.; Lu, Y.; Chia, A.; Zhang, M.; Rupar, P. A.; Gunari, N.; Walker, G. C.; Cambridge, G.; He, F.; Guerin, G. Self-seeding in one dimension: a route to uniform fiber-like nanostructures from block copolymers with a crystallizable core-forming block. *ACS nano* **2013**, 7 (5), 3754-3766.
22. Qian, J.; Li, X.; Lunn, D. J.; Gwyther, J.; Hudson, Z. M.; Kynaston, E.; Rupar, P. A.; Winnik, M. A.; Manners, I. Uniform, high aspect ratio fiber-like micelles and block co-micelles with a crystalline  $\pi$ -conjugated polythiophene core by self-seeding. *J. Am. Chem. Soc.* **2014**, 136 (11), 4121-4124.
23. Li, X.; Jin, B.; Gao, Y.; Hayward, D. W.; Winnik, M. A.; Luo, Y.; Manners, I. Monodisperse Cylindrical Micelles of Controlled Length with a Liquid-Crystalline Perfluorinated Core by 1D "Self-Seeding". *Angew. Chem. Int. Ed.* **2016**, 55 (38), 11392-11396.
24. Hsiao, M.-S.; Zheng, J. X.; Van Horn, R. M.; Quirk, R. P.; Thomas, E. L.; Chen, H.-L.; Lotz, B.; Cheng, S. Z. D. Poly(ethylene oxide) Crystal Orientation Change under 1D Nanoscale Confinement using Polystyrene-block-poly(ethylene oxide) Copolymers: Confined Dimension and Reduced Tethering Density Effects. *Macromolecules* **2009**, 42 (21), 8343-8352.
25. Inam, M.; Jones, J. R.; Perez-Madrigal, M. M.; Arno, M. C.; Dove, A. P.; O'Reilly, R. K. Controlling the Size of Two-Dimensional Polymer Platelets for Water-in-Water Emulsifiers. *ACS. Cent. Sci* **2018**, 4 (1), 63-70.
26. Massey, J. A.; Temple, K.; Cao, L.; Rharbi, Y.; Ruez, J.; Winnik, M. A.; Manners, I. Self-assembly of organometallic block copolymers: the role of crystallinity of the core-forming polyferrocene block in the micellar morphologies formed by poly (ferrocenylsilane-b-dimethylsiloxane) in n-alkane solvents. *J. Am. Chem. Soc.* **2000**, 122 (47), 11577-11584.
27. Tritschler, U.; Gwyther, J.; Harniman, R. L.; Whittell, G. R.; Winnik, M. A.; Manners, I. Toward Uniform Nanofibers with a  $\pi$ -Conjugated Core: Optimizing the "Living" Crystallization-Driven Self-Assembly of Diblock Copolymers with a Poly(3-octylthiophene) Core-Forming Block. *Macromolecules* **2018**, 51 (14), 5101-5113.
28. Shin, S.; Menk, F.; Kim, Y.; Lim, J.; Char, K.; Zentel, R.; Choi, T. L. Living Light-Induced Crystallization-Driven Self-Assembly for Rapid Preparation of Semiconducting Nanofibers. *J. Am. Chem. Soc.* **2018**, 140 (19), 6088-6094.

29. Yu, W.; Inam, M.; Jones, J. R.; Dove, A. P.; O'Reilly, R. K. Understanding the CDSA of poly (lactide) containing triblock copolymers. *Polym. Chem.* **2017**, 8 (36), 5504-5512.
30. Petzetakis, N.; Walker, D.; Dove, A. P.; O'Reilly, R. K. Crystallization-driven sphere-to-rod transition of poly (lactide)-b-poly (acrylic acid) diblock copolymers: mechanism and kinetics. *Soft Matter* **2012**, 8 (28), 7408-7414.
31. Song, Y.; Chen, Y.; Su, L.; Li, R.; Letteri, R. A.; Wooley, K. L. Crystallization-driven assembly of fully degradable, natural product-based poly (l-lactide)-block-poly ( $\alpha$ -d-glucose carbonate) s in aqueous solution. *Polymer* **2017**, 122 (3), 270-279.
32. Li, Z.; Sun, L.; Zhang, Y.; Dove, A. P.; O'Reilly, R. K.; Chen, G. Shape effect of glyco-nanoparticles on macrophage cellular uptake and immune response. *ACS Macro Lett.* **2016**, 5 (9), 1059-1064.
33. Du, Z.-X.; Xu, J.-T.; Fan, Z.-Q. Micellar Morphologies of Poly ( $\epsilon$ -caprolactone)-b-poly (ethylene oxide) Block Copolymers in Water with a Crystalline Core. *Macromolecules* **2007**, 40 (21), 7633-7637.
34. Du, Z. X.; Xu, J. T.; Fan, Z. Q. Regulation of Micellar Morphology of PCL - b - PEO Block Copolymers by Crystallization Temperature. *Macromol. Rapid Commun.* **2008**, 29 (6), 467-471.
35. Ganda, S.; Dulle, M.; Drechsler, M.; Förster, B.; Förster, S.; Stenzel, M. H. Two-Dimensional Self-Assembled Structures of Highly Ordered Bioactive Crystalline-Based Block Copolymers. *Macromolecules* **2017**, 50 (21), 8544-8553.
36. Rizis, G.; van de Ven, T. G.; Eisenberg, A. "Raft" Formation by Two - Dimensional Self - Assembly of Block Copolymer Rod Micelles in Aqueous Solution. *Angew. Chem. Int. Ed.* **2014**, 53 (34), 9000-9003.
37. Arno, M. C.; Inam, M.; Coe, Z.; Cambridge, G.; Macdougall, L. J.; Keogh, R.; Dove, A. P.; O'Reilly, R. K. Precision Epitaxy for Aqueous 1D and 2D Poly( $\epsilon$ -caprolactone) Assemblies. *J. Am. Chem. Soc.* **2017**, 139 (46), 16980-16985.
38. He, W.-N.; Zhou, B.; Xu, J.-T.; Du, B.-Y.; Fan, Z.-Q. Two Growth Modes of Semicrystalline Cylindrical Poly( $\epsilon$ -caprolactone)-b-poly(ethylene oxide) Micelles. *Macromolecules* **2012**, 45 (24), 9768-9778.
39. Wang, X.-Y.; Wang, R.-Y.; Fan, B.; Xu, J.-T.; Du, B.-Y.; Fan, Z.-Q. Specific Disassembly of Lamellar Crystalline Micelles of Block Copolymer into Cylinders. *Macromolecules* **2018**, 51 (5), 2138-2144.
40. Yang, J.-X.; Fan, B.; Li, J.-H.; Xu, J.-T.; Du, B.-Y.; Fan, Z.-Q. Hydrogen-Bonding-Mediated Fragmentation and Reversible Self-assembly of Crystalline Micelles of Block Copolymer. *Macromolecules* **2015**, 49 (1), 367-372.
41. Wang, J.; Zhu, W.; Peng, B.; Chen, Y. A facile way to prepare crystalline platelets of block copolymers by crystallization-driven self-assembly. *Polymer* **2013**, 54 (25), 6760-6767.
42. Todo, M.; Park, S.-D.; Takayama, T.; Arakawa, K. Fracture micromechanisms of bioabsorbable PLLA/PCL polymer blends. *Engineering Fracture Mechanics* **2007**, 74 (12), 1872-1883.
43. Inam, M.; Cambridge, G.; Pitto-Barry, A.; Laker, Z. P. L.; Wilson, N. R.; Mathers, R. T.; Dove, A. P.; O'Reilly, R. K. 1D vs. 2D shape selectivity in the crystallization-driven self-assembly of polylactide block copolymers. *Chem. Sci.* **2017**, 8 (6), 4223-4230.
44. Su, M.; Huang, H.; Ma, X.; Wang, Q.; Su, Z. Poly(2-vinylpyridine)-block -Poly(-caprolactone) single crystals in micellar solution. *Macromol. Rapid Commun.* **2013**, 34 (13), 1067-1071.

Length control of biodegradable fibre-like micelles *via* tuning solubility: a self-seeding Crystallization-Driven Self-Assembly of poly( $\epsilon$ -caprolactone) containing triblock copolymers

Wei Yu†, Jeffrey C. Foster§, Andrew P. Dove\*§ and Rachel K. O'Reilly\*§

